Phase-Transition Microneedle Patches for Efficient and Accurate Transdermal Delivery of Insulin

*Sixing Yang, Fei Wu, Jianguo Liu, Guorong Fan, William Welsh, Hua Zhu, and Tuo Jin**

Utilizing the unique virtue of polyvinyl alcohol (PVA) of forming microcrystalline domains as the cross-linking junctions, a new microneedle system, phase-transition microneedle (PTM) patch, is invented, which enables highly efficient transdermal delivery of insulin without depositing the needle tip materials to the skin. PTM, formed of biocompatible PVA as the main component, is sufficiently strong for its needle tip to penetrate the epidermis in the dry state, release preloaded cargos by absorbing body fluid in the dermis layer nearly as fast as subcutaneous injection, and retain mechanical toughness in the hydrated state to ensure complete removal from the skin. The microcrystalline cross-linking enables a protein-friendly fabrication process free of hazardous cross-linking agents required for chemical and ionic cross-linking. Pharmacokinetic and efficacy studies of insulin-loaded PTM using pig models indicate a transdermal bioavailability over 20%, similar deviations and peak width, only 18 min behind Tmax, and lower glycated hemoglobin (HbA_{1c}) as compared with injection pens. The complete removability of hydrated needle tips may endow PTM with an additional safety insurance, terminating medication whenever hypoglycemia becomes a concern. PTM patch is practically applicable to a variety of protein/peptide medicines requiring frequent dosing by offering painless administration, freedom of refrigeration, and minimal safety concerns.

1. Introduction

Efficient and precise noninvasive dosing of insulin has been a long-standing challenge that has attracted extensive research efforts and has witnessed many technical achievements over the past half century.[1] The reported approaches comprise nanoparticles for oral absorption,[2] microparticles for inhalation,[3,4] mucosal spray for bulk uptake,[5] needleless high pressure injection,[6] as well as chemical enhancer and thermal abrasion aided skin permeability promotion.[7] Among these strategies, microneedles, first reported in 1998,[8] demonstrate the most feasible solution to date for noninvasive delivery of insulin, a protein medicine being administrated on a recurrent basis (often multiple doses per day) and within a narrow efficacy–toxicity window to tens millions of patients.[9,10]

Microneedles are an array of small needles, up to 1 mm in length, which penetrate and create diffusion channels through the epidermis without causing skin injury or feeling of pain. The microneedles reported in the literature can be categorized as solid microneedles,[11–13] hollow microneedles,[14,15] and dissolvable (or degradable) microneedles.[16,17] Solid microneedles are able to create transient channels across the epidermis, but lack the capacity to load medicines. Although coating on the surface of solid microneedles presents a strategy to deliver medicines of low dose (limited to several tens of micrograms) through the skin,[13] the delivery of insulin which normally requires at least 360 μm per dose would not be feasible. Hollow microneedles would seem an ideal design for microinjection, but face issues with fabrication complexity, insufficient mechanical strength, blocking by dermal tissues,[2–4] and the need for suboptimal injection driving force.[15,18] While dissolvable microneedles (DMs) and top-off microneedles[19] may solve the problems above and feasible to be incorporated into a dermal patch,[16] deposition of the needle tip materials to skin raises concerns for delivering medicines that require frequent administration for prolonged time periods (such as insulin).[20,21] An experiment on rat model indicated that the scars on the skin caused by dissolvable hyaluronic acid (HA) microneedles retained 72 h after removal of the patch.[21] Although the polymers employed for fabricating DMs have long-established safety profiles, their intradermal reabsorption has yet to be reported. In addition, since needle dissolution allows all the substances contained to be released to the dermis layer, sterilization has to be achieved

Dr. S. Yang, Dr. F. Wu, Prof. T. Jin
School of Pharmacy
Shanghai Jiao Tong University
800 Dongchuan Road, Shanghai 200240, China
E-mail: tomtjin@gmail.com
Prof. J. Liu, Prof. G. Fan
School of Pharmacy
Second Military Medical University of PLA
325 Guohe Road, Shanghai 200433, China
Prof. W. Welsh
Department of Pharmacology
Rutgers University
Robert Wood Johnson Medical School
661 Hoes Lane West, Piscataway, NJ 08854, USA
Prof. H. Zhu
Department of Microbiology and Molecular Genetics
Rutgers University
New Jersey Medical School
Newark, NJ 07101, USA

DOI: 10.1002/adfm.201500554

© 2015 WILEY-VCH Verlag GmbH & Co. KGaA, Weinheim

by using a costly aseptic facility covering the entire fabrication process.

More recently, hydrogel forming microneedles (HFMs) are able to release hydrophilic cargos by swelling (instead of dissolving) in the dermis layer and to be withdrawn from the skin completely by virtue of the toughness of their cross-linked matrix.[16,22] However, the antidissolution cross-linking is achieved by covalent bond as the cross-linking junctions through postmolding chemical reaction, which may expose the protein medicines to hazardous chemicals and conditions if loaded prior to molding.[23] Cross-linking agents or multivalent ions that, respectively, induce the covalent junctions[16,22] or bridge the ionic cross-linking[19] may interact with susceptible proteinaceous biomolecules loaded in the microneedle matrix. Alternatively, loading the protein medicine at the back of the microneedle array postmolding may result in insufficient efficacy due to the extended diffusion pathway.[22] An HFM patch carrying 62 IU postmolding-loaded insulin (a dose equivalent to several injections for a human) lowered the glucose level of a diabetic rat for only 10% at 2 h point and 63% (including the sugar drop by starvation) at 12 h point postadministration (**Figure 1**A,B).[22] To achieve sufficient efficacy, an electrode was applied together with the microneedles to the animal skin to afford iontophoresis-assisted delivery.[22]

All these aforementioned microneedle strategies have contributed substantially to the development of a microneedle patch that is capable of offering sufficient capacity to load biologics in their native state, efficient and accurate doses, ease of production, and freedom from needle material deposition. Notwithstanding this technological progress, it appears that no single microneedle patch satisfies all of these criteria.

In this article, we describe a new microneedle system called the phase-transition microneedle (PTM) patch that is designed from a common pharmaceutical excipient, polyvinyl alcohol (PVA), to form the matrix of the microneedles. PVA has excellent biocompatibility and chemical inertness and, more importantly, it forms micro- or submicrocrystalline domains as the cross-linking junctions of its polymeric networks during temperature change.[24] This mechanism enables the postmolding cross-linking be achieved by a freeze-thaw treatment under a mild condition compatible to biologics, so that insulin can easily be loaded in the microneedle matrix to achieve therapeutically sufficient transdermal delivery without denaturing. The design and working principle of a PTM patch is depicted in Figure 1A,B. The needle tips are sufficiently hard in the dry glassy state to penetrate the epidermis, convert to a water-swollen hydrogel state by absorbing interstitial fluid in the dermis layer to release the insulin preloaded in the needle tip matrix efficiently, and maintain their toughness at the hydrated state through the microcrystalline cross-linking junctions to ensure complete removal from the skin (Figure 1B).

The fabrication process of the PTM patch (Figure 1C) consists a series of simple unit operations: i) load the drug-containing PVA-dominated polymer solution on a mold, ii) indraft the polymer solution into the arrayed microholes of the mold by vacuum, iii) freeze-thaw the molded polymer solution to form the microcrystalline domains as the cross-linking junctions,[25] iv) detach from the mold and dry, v) steam the dried microneedle sheets in oxirane vapor for sterilization, and vi) punch the dried microneedle sheet to designed size and pack the punched microneedle patches in moisture-proof bags. This process may offer two cost-efficient features absent for DMs: 1) the mold may return to the production cycle since the freeze-thawed microneedle sheet is removable from it; 2) sterilization may be achieved by steaming the final product in an oxirane vapor to avoid an aseptic facility for the whole process since bacteria particles, if there are some in the needle tips, cannot be released.

The microcrystalline cross-linking design offers sufficient mechanical strength for removal of the microneedles in the hydrated state while, at the same time, avoids exposing the biologic therapeutics to reactive and multi-ionic agents used in covalent and ionic cross-linking.[19,23] The density of the micro- or submicrocrystalline cross-link junctions in the network, a factor that controls the water-swelling ratio and drug release rate, may easily be adjusted by the cycles of the freeze-thaw treatment.[26] In addition to freeze-thaw cycles, the drug diffusion channels may also be enriched by blending polysaccharides into the PVA phase. The blended polysaccharides become dispersed in the PVA matrix during the process of freeze-thaw treatment and drying, and offer multiple functions such as partition reservoirs, cryoprotectors, and diffusion channels for protein and peptide drugs. The microneedles used in the efficacy and pharmacokinetic studies of this report comprised 85% PVA, 10% dextran, and 5% carboxymethylcellulose (CMC). The dimensions were 0.85 mm in length and 0.28 mm in base diameter.

2. Results

2.1. Swelling, Skin Insertion, and Recovery

A prototype PTM patch, 12 mm in diameter, possesses ≈135 needle tips, 0.85 mm in length (**Figure 2**A). Pressing a (insulin free) microneedle patch on live human skin with an adhesive backing film (3M 9860) for 3 h (Figure 2E) resulted in a significantly swollen patch as desired (Figure 2B). The swollen microneedles were all withdrawn from the skin without breakage or damage (Figure 2B). If, instead, the same microneedle patch is pressed on the skin of the same volunteer under identical conditions after all the needle tips were excised, the swelling was much less (compare Figure 2B,C). The different swollen states of the patches in Figure 2B,C lead to two conclusions: 1) the PTM tips penetrated the epidermis and reached the dermis interstitial fluid of human skin; and 2) the dermis fluid was sufficient to swell the microneedles through the needle tips. Complete removal of the swollen microneedles, as shown in Figure 2B, offers two additional advantages: absence of needle material deposition in the skin, and flexibility to terminate treatment if adverse drug reactions or overdose (often seen for insulin administration) becomes a concern.

Resistance of the PVA needle tips of PTM to static and dynamic forces was compared with two well-reported polysaccharide DMs, CMC microneedles and HA microneedles through two quick experiments. When weights of gradually increased mass were gently placed onto the microneedle arrays, 26 mm^2 in area (an array of 5×6 microneedles), consequently

© 2015 WILEY-VCH Verlag GmbH & Co. KGaA, Weinheim

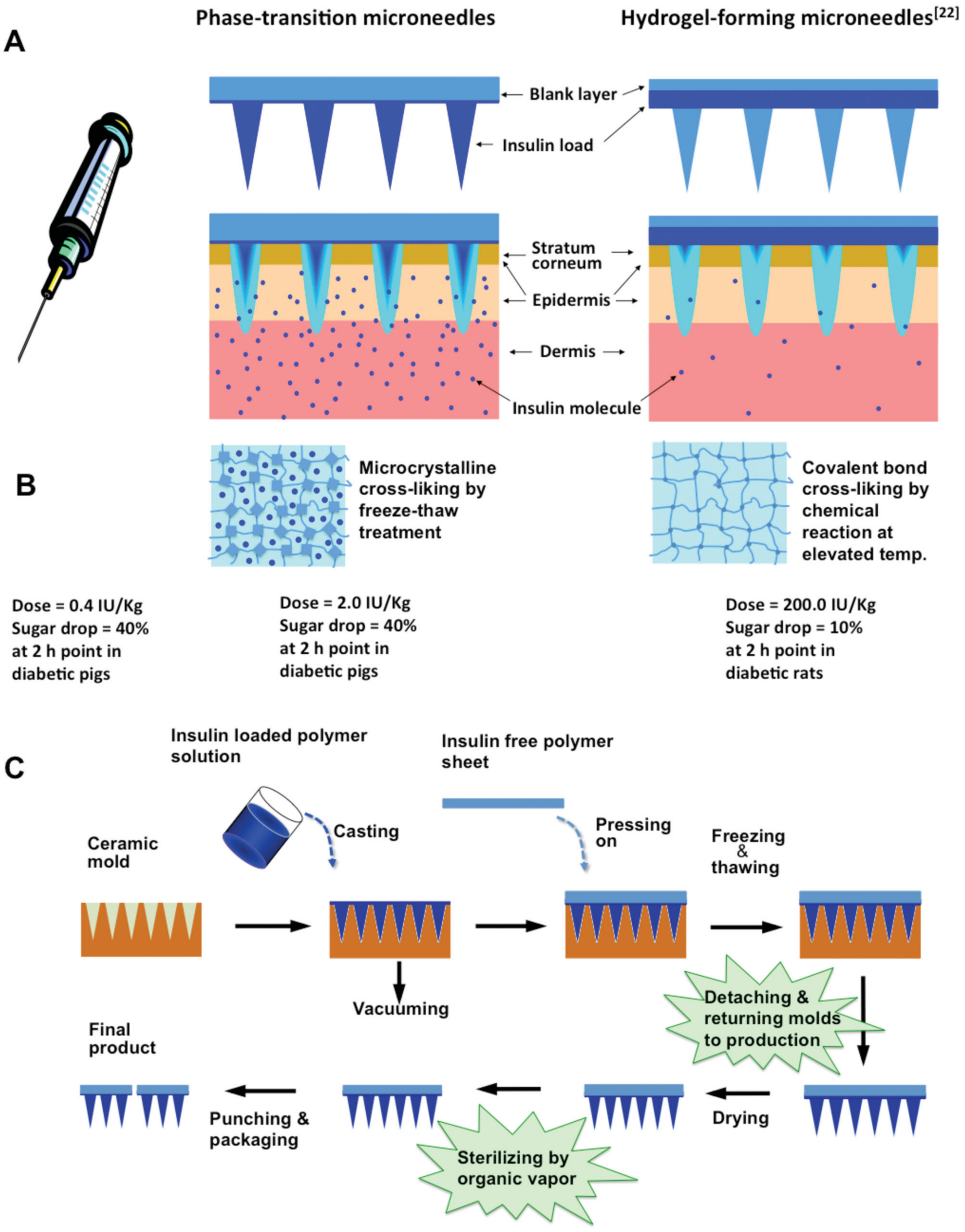

Figure 1. Working principle and fabrication process of PTM patches. A) The microneedles absorb the bodily fluid from the dermis layer to convert form hard glassy state to hydrogel state to allow the preloaded insulin to release to the bodily fluid in the dermis layer. B) The microneedle matrix of PTM is cross-linked to avoid dissolution through microcrystalline domains as the cross-linking junctions via a freeze-thaw treatment while that of HFM is cross-linked through covalent bands as the cross-linking junctions via a chemical reaction. Therefore, insulin can be loaded in the needle tips of PTM to achieve a relative bioavailability of 20%, while insulin has to be loaded at the back of the microneedle array of HFMs that leads to a bioavailability less than 1% due to the extended diffusion pathway. C) The PTM patch may be fabricated using a scalable process comprising a sequence of simple unit operations involving circulation of the molds in the production line and sterilization of the final product by steaming in oxirane vapor.

at room temperature and 55% humidity, the weights that caused failure of the needle tips were 230, 450, and 450 g for the CMC, HA, and PVA microneedles, respectively. The microneedles of all the three patches remained intact when a balance weight of 20 g was dropped onto them from a height of 20 mm, but failed when the weight was increased to 50 g. Since the PTM patch used in the present study was a rounded disk 12 mm in diameter (113 mm^2 in area), it should tolerate 2 kg static force and a dynamic impact by a 100 g weight from 20 mm height. For hardness test, the solid testing-weight was supported by 30 microneedle tips. In the case of skin test, however, the force was distributed to the tips and shaft of 135 microneedles due to deformation of the soft skin. Although the above test may not be precise, the comparative study indicates that the PVA-based needle tips of PTM are at least equivalent to the CMC and HA microneedles in resisting static pressure and dynamic impact. The latter have been reported to be strong enough to penetrate the epidermis and enable transdermal delivery of insulin.[21,27]

© 2015 WILEY-VCH Verlag GmbH & Co. KGaA, Weinheim

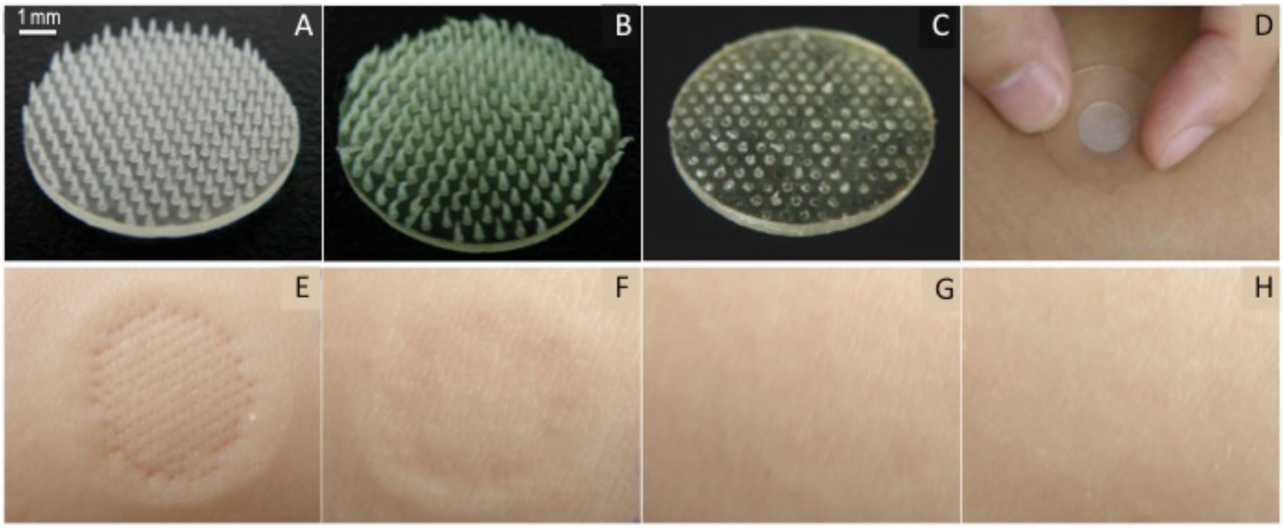

Figure 2. Characteristics of phase-transition hydrogel microneedle patches. A) Dry microneedle patch with an array of needles 0.85 mm in length and 0.28 mm in base diameter. B) Swollen microneedle patch applied on live human skin for 3 h. C) The same microneedle patch applied on the same volunteer after all the needle tips were excised. D) Microneedle patch being pressed on live human skin with an adhesive backing membrane. E) Spot on human skin right after detachment of the microneedle patch. F,G,H) The same spot of human skin 15, 120, and 300 min after detachment of the microneedle patch.

Skin compatibility of the inert, insoluble, and hydrophilic PTM microneedles was examined by recovery rate of the skin spot of volunteers after the drug-free patches were attached for 3 h (Figure 2D). Prior to applying the patch, the site of the skin of each volunteer was cleaned using 75% alcohol and dried in air. Photographs were taken concurrently as a function of the time since the patch was removed from the skin (using Olympus camera, Sp-565uz, JP). Removal of the microneedle patch revealed an impression of the array of microholes created by the needle tips on the skin (Figure 2E). These microholes became invisible 15 min after removal of the patch (Figure 2F), and the impression was vaguely visible 120 min after removal of the patch (Figure 2G). At 300 min since removal of the patch, the spot of the skin where the microneedle patch was applied was completely recovered under the camera (Figure 2H). Rashes, clear erythema, or itching feeling were not observed or experienced among the human volunteers. These observations suggest that PTM patches are suitable for frequent administration of medicines via transdermal route.

2.2. Pharmacokinetics and Dosing Accuracy

To determine the bioavailability and pharmacokinetics parameters of the insulin patch, Bama pigs 10–12 kg in body weight were treated by this transdermal dosage form at three different doses. Normal pigs were divided into three groups (6 in each) and attached with 1 (1.0 IU kg^{-1}), 2 (2.0 IU kg^{-1}), and 3 (3.0 IU kg^{-1}) microneedle patches on their ears, respectively. For comparison, another group of six pigs was given an insulin injection at the dose of 0.4 IU kg^{-1} (Eli Lilly's injection pen). Prior to drug administration, the basal blood insulin of each pig was monitored for 1 h, followed by attachment of an insulin-free microneedle patch to establish the insulin baseline. The basal and postadministration blood insulin were both monitored for 8 h using ELISA (R&D Systems, USA). The insulin content of blood samples taken from the test animals was measured using ELISA. The measured postdosing blood insulin was subtracted by the basal insulin at each corresponding data point and plotted against time (**Figure 3**A). The blood insulin of the pigs that received three different doses of microneedle patches showed correlated dose-dependent profiles. The area under the curve (AUC) values of the blood insulin profiles were 719 ± 211, 1055 ± 71, and 1541 ± 171 min ng^{-1} mL^{-1} for the pigs attached with one, two, and three insulin patches, respectively. The blood concentration of insulin reached maximum around 60 min after the patches were applied (Figure 3A,B), approximately the same as the peak of postmeal sugar.

Among the tested pigs, the AUC was comparable for those attached with the two insulin patches (dose: 2.0 IU kg^{-1}) (1055 ± 71 min ng^{-1} mL^{-1}) to those given a shot of the injection pen (dose: 0.4 IU kg^{-1}; AUC: 1155 ± 114 min ng^{-1} mL^{-1}) (Figure 3A). Based on this result, diabetic pigs receiving either two microneedle patches or a shot of injection pen were compared with each other. The AUCs of insulin in the two groups of diabetic pigs were 1006 ± 126 and 962 ± 227 min ng^{-1} mL^{-1}, respectively (Figure 3B). Comparisons between the AUC values, resulting from two microneedle patches or a shot of injection pen in the cases of both normal and diabetic pigs (Figure 3A,B), suggest that the relative bioavailability of the insulin microneedle patch in pigs was 20% on the basis of total insulin loaded in the microneedles.

Another important note was that the standard deviations of the blood insulin curves for the pigs receiving microneedle patches or injection pens were comparable to each other (Figure 3A,B). This outcome suggests that PTM patches may offer insulin dosing of predictable accuracy as that of injection pens. Further analysis of the blood insulin profiles revealed that the onset peak of the microneedle patch was ≈20 min behind that of the injection pen, followed by a low concentration

© 2015 WILEY-VCH Verlag GmbH & Co. KGaA, Weinheim

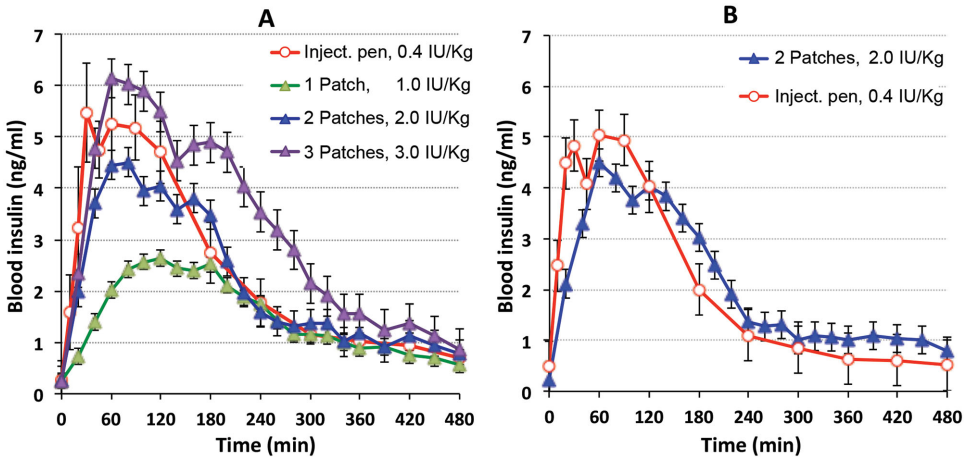

Figure 3. Pharmacokinetic profiles of insulin in pig models received insulin microneedle patches or insulin injection pen. A) Dose dependency of blood insulin profiles in normal pigs (6 in each group). B) Blood insulin profiles in diabetic pigs (6 in each group).

insulin profile in next 3 h (Figure 3B). This sustained release capability may be beneficial for control of basal blood sugars. The peak width of the initial surge of the blood insulin by the PTM patch was comparable to that of the injection pen (Figure 3), suggesting that the transdermal dosage form should not result in significant over dose and hypoglycemia.

2.3. Pharmacodynamics

The efficacy of the insulin-loaded PTM patch was examined by three standard experiments on diabetic pigs: A) giving insulin formulations after 12 h fasting and measuring blood sugar level 2 h after drug administration; B) injecting glucose (0.6 g kg^{-1}) immediately after insulin administration then monitoring blood sugar level as a function of time; and C) measuring glycosylated hemoglobin after continuous insulin treatment for 2 months (**Figure 4**). The diabetic models were created by surgical removal of 75% pancreas of Bama pigs and confirmed by measuring blood sugar continuously for 2 weeks. Each of the test groups consisted of six pigs, 11–12 kg in body weight. The blood sugar level in the fasting pigs at the 2 h point after insulin administration dropped correspondently with the dose of the PTM patch (Figure 4A). The diabetic pigs that received two insulin patches (2.0 IU kg^{-1}) or injection pen (0.4 IU kg^{-1}) showed comparable blood sugar drop, consistent with the pharmacokinetics result that the AUC of the two groups was similar (Figure 3B).

For the sugar tolerance experiment (Figure 4B), injection of 0.6 g kg^{-1} glucose in the pigs that received no insulin treatment triggered an increase in blood sugar followed by a gradual decline after 1 h. For the pigs given a shot by injection pen, the blood sugar level declined immediately and reached the minimum (12 mmol L^{-1}) at 2 h postinsulin dosing after which the blood sugar proceeded to rebound toward the original level. The pigs treated with different doses of insulin patches showed dose-dependent blood sugar profiles. The blood sugar concentrations in the diabetic pigs gradually dropped to 17, 12, and 9 mmol L^{-1} in 2 h after one, two, and three insulin patches (equivalent to 1.0 IU kg^{-1}, 2.0 IU kg^{-1}, and 3.0 IU kg^{-1} of doses) were given to each pig of the test groups, respectively (Figure 4B). Compared with the pigs injected with insulin subcutaneously using injection pens, blood sugars in those receiving microneedle patches dropped slowly within the initial

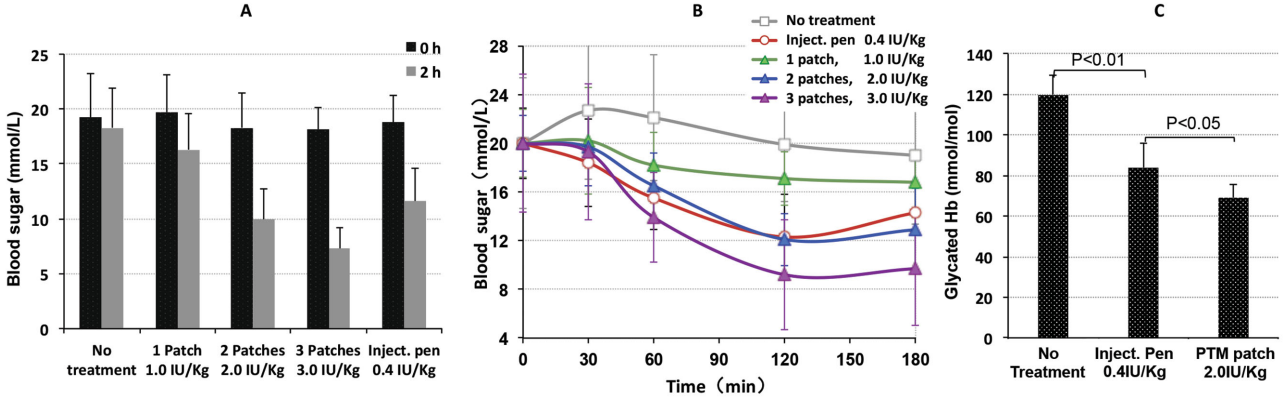

Figure 4. Hypoglycemic efficacy of insulin PTM patches in comparison with insulin injection pen. A) Hypoglycemic rate 2 h after administration of various insulin dosage forms to diabetic pigs fasted for 12 h. B) Hypoglycemic profiles in diabetic pigs receiving 0.6 g kg^{-1} glucose injection and various insulin dosage forms at the same time. C) Levels of glycated hemoglobin in diabetic pigs after being treated with various insulin dosage forms for 2 months.

© 2015 WILEY-VCH Verlag GmbH & Co. KGaA, Weinheim

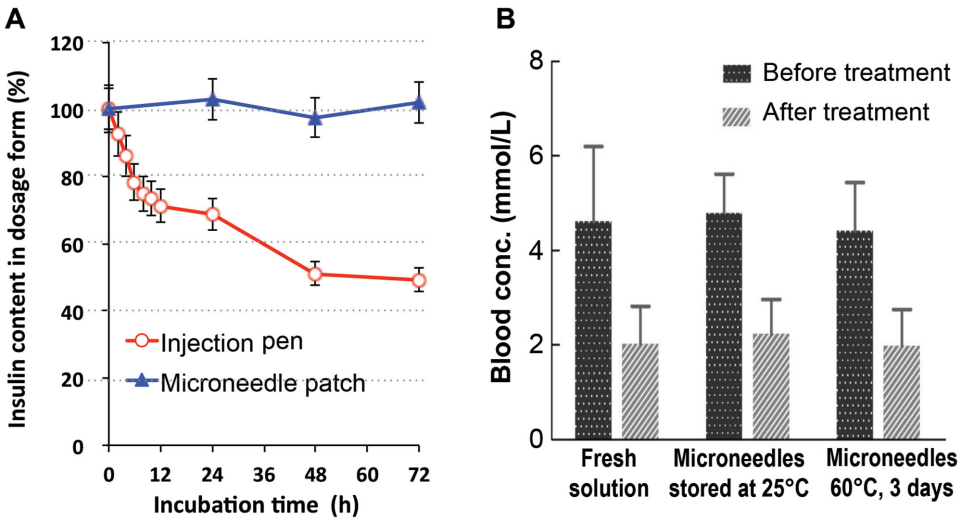

Figure 5. Stability of insulin microneedle patches and insulin injection pen at elevated temperature. A) Changes in insulin content as a function of baking time at 60 °C. B) Hyperglycemic activity of the insulin recovered from the baked and unbaked microneedle patches.

30 min, but reached the minimum at the same time (2 h) after insulin administration. Unlike the injection pen group, the blood sugar concentration for the microneedle groups did not rebound at the 2 h point, but remained at the low level for at least another hour (Figure 4B). The profiles of hypoglycemic efficacy of the insulin dosage forms shown in Figure 4B are consistent with the blood insulin profiles shown in Figure 3. Among the pigs that received microneedle patches, those given two patches of dose (2.0 IU kg^{-1}) showed the same minimal blood sugar level as those treated by injection pen (0.4 IU kg^{-1}). The similarities in hypoglycemic efficacy between the doses of 2.0 IU kg^{-1} microneedle patch and 0.4 IU kg^{-1} injection pen reflect the similarity of the AUC of blood insulin between the two pig groups that received the same two dosage regimens, respectively (Figure 3B).

2.4. Glycated Hemoglobin (Efficacy of Long-Term Therapy)

To examine the efficacy of the insulin microneedle patch for prolonged blood sugar control, the diabetic pigs were treated with insulin continuously for 2 months, followed by measurement of HbA1c which is a form of hemoglobin that serves as a marker to identify the average plasma glucose concentration over prolonged periods of time. In diabetes mellitus, higher levels of HbA1c indicate poorer control of blood glucose levels. The level of HbA1c in the pigs that received various treatments was measured by ELISA kit (Jiancheng Tech Co. Ltd, Nanjing, China). The HbA1c level in the untreated diabetic pigs was as high as 120 mmol mol^{-1}, an index signaling diabetic condition (Figure 4C). For the pigs that received either the insulin injection pen (0.4 IU kg^{-1}) or microneedle patch (2.0 IU kg^{-1}) for 2 months, the HbA1c level dropped to 84 and 69 mmol mol^{-1}, respectively. Although the insulin injection and microneedle patch exhibited the same blood insulin AUC (Figure 3B), the latter showed significantly better control of long-term blood glucose as measured by HbA1c level. This advantage of the PTM patches is probably due to their post-peak sustained release of insulin (Figures 3B and 4C).

2.5. Stability

PTM patches may prevent loaded proteins from denaturing due to temperature changes, a key advantage for protein medicines to avoid cold chain refrigeration. To demonstrate this capability, insulin-loaded PTM patches were incubated together with a solution formulation at 60 °C for 3 d, followed by an HPLC (high performance liquid chromatography) analysis for insulin content and an animal assay for hypoglycemic activity. After 72 h incubation at 60 °C, monitoring of the insulin content revealed a 53% loss for the solution formulation, but no change in insulin content for the microneedle patch (**Figure 5**A). Significantly, the hypoglycemic activity of the insulin extracted from the incubated patches was equivalent to fresh insulin and unbaked PTM patch (Figure 5B). The protein stabilization effect of the hydrophilic glassy matrix of the microneedle patches not only protects insulin against heat but also prevents it from denaturing by ice-forming freezing, making refrigerating and antifreezing of insulin formulations unnecessary.

3. Discussion

3.1. The Material Nature of PVA

The defining attribute of the PTM patch, viz., the ability to load insulin in the matrix of swellable-but-insoluble microneedle tips without the concern of denaturing, is ensured by the unique material nature of PVA. Specifically, the PVA chains undergo microcrystalline cross-linking to gel its solution by mild treatment (freeze-and-thaw).[28] Its aliphatic [—C—C—] backbone, together with its ability to form microcrystalline domains through interchain hydrogen bonding via its —OH groups, renders PVA chemically resistant, highly hydrophilic, biocompatible, and mechanically strong and elastic at both dry and hydrated states. A PVA hydrogel implant remained intact with no surface deposition after being implanted in rats for 3 months.[29] The density of the microcrystalline domains of PVA

© 2015 WILEY-VCH Verlag GmbH & Co. KGaA, Weinheim

may be adjusted by controlling the cycles of the freeze-thaw treatment and/or blending polysaccharides in the PVA solution, convenient and mild means to optimize the desired balance between mechanical strength and drug permeability of a PVA device.

Due to its unique features, PVA is widely used in both medicine as a biocompatible excipient[28] and in engineering as a high-strength hydrophilic fiber material.[30] For microneedle facilitated transdermal drug delivery, PVA possesses advantages over other microneedle forming materials. Unlike silicon, metal, and glass microneedles, the PVA-based PTM needle tips change from hard glass to soft and elastic hydrogel post-application, a material state having the least discomfort sensation in the skin and suitable for relative long-term in-skin release (Figure 2E–H). For a microneedle patch formed of dissolvable HA, the specks of the holes caused by the needle tips on the rat skin remained visible over 72 h after removal of the patch.[20] The interchain cross-linking endows the PTM microneedles with sufficient mechanical strength to penetrate epidermis at dry state and withdraw from the skin at hydrated states (Figure 2A–D) without depositing needle tips materials in the skin. The water-swelling capability offers a mechanism for efficient transdermal protein/peptide delivery with predictable accuracy (Figure 3A,B). Finally, its microcrystalline cross-linking and hydrophilic matrix ensures protein stability in both formulation and storage (Figures 1B and 4).

3.2. Release Kinetics and Bioavailability

An important advantage of the PTM patch over other polymeric microneedles is its flexibility of design to achieve various release profiles of insulin. Currently available insulin dosage regimes involve fast-acting injections to treat the postmeal surge of blood sugar, sustained-release injections to control the basal blood sugar level, and premixed formulations of the above two to meet the two therapeutic needs by one dose. To achieve these insulin-dosing profiles, a microneedle patch must satisfy both criteria, i.e., maintaining a persistent cross-epidermal pathway over the desired dosing period and enabling insulin to be loaded in the matrix of the needle tips in sufficient amount. While hydrogel-forming microneedles and DMs meet one of these two criteria, PTM satisfies both of them simultaneously. Its protein-friendly microcrystalline cross-linking (to prevent needle tip dissolution) allows proteins to be preloaded in the needle tips without the concerns of denaturing during post-molding cross-linking, and its water swellable-but-insoluble needle tips are able to sustain the cross-epidermis diffusion channels for insulin over the entire doing period when applied on the skin.

For DMs patches, a study on relative pharmacologic availability (RPA) indicated that limiting the insulin loading to the front half of the needle tips instead of the entire microneedle shaft resulted in an increase in RPA from 9.2% to 30.7% in diabetic rats.[27] Further analysis revealed that 18.4% of the total insulin loaded in the entire tips of DM, twice as its in vivo RPA, was released due to the needle dissolution.[27] The discrepancy between the fraction of release and in vivo RPA suggests that the cross-epidermis channels created by the dissolving chondroitin microneedles closed before most of the dissolved insulin could pass through. In the present study, the relative availability of insulin delivered by the PTM to diabetic pigs (which have a thicker epidermis than rats) was over 20% of the total insulin loaded along the entire microneedle shafts. By the virtue of its swellable-but-insoluble needle tips, the PTM can accommodate the three popular insulin-dosing regimens (fast acting, sustained release, and their combination) by loading insulin in selected regions along the microneedle shafts (in the front of tips, mainly in the base, and in the entire body). Importantly, PTM does not deposit needle tip material in the skin.

DM made of an anionic polysaccharide, HA, was reported to show over 90% RPA in diabetic rats for full-needle insulin loading,[21] nearly five times higher than that of the disaccharide chondroitin DM.[27] Although not discussed in this article, the difference in RPA between the two similar DMs suggests that the less diffusible polysaccharide HA dissolved from the microneedles was retained in the epidermis for a longer period of time and served as sustained diffusion channels for the insulin loaded in the basal half of the microneedle shaft (the section not contacting with the epidermis fluid directly). The notion that dissolved HA microneedles persisted across the epidermis is supported by the prolonged specks of the holes caused by the microneedles on the rat skin reported by the same researchers.[20] The ability of the hydrated HA phase to facilitate insulin diffusion implies that blending sufficient, yet not too much to prevent PVA cross-linking, anionic polysaccharides into the network of the PTM microneedles may be a useful strategy to improve the insulin bioavailability from the PTM patch.

3.3. The Fabrication Process

The usage of the air-permeable but water-impermeable mold allows a scalable fabrication process to be designed by applying a vacuum at the backside of the mold to suck the microneedle-forming polymer solution into the microholes. Unlike the reported polymer casting methods using centrifugation or a vacuum chamber to enforce the microhole filling, the present process can easily be incorporated into a production line covered by a sterile hood. The ability of the PVA-based microneedles to form microcrystalline domains as the cross-linking junctions through a postmolding freeze-thaw treatment may endow the casted PTM patch with sufficient mechanic strength to detach from the mold for off-mold drying and punching, by which the molds can return to the production line and the number of molds required may be reduced. Moreover, the swelling but insoluble needle tip of PTM allows only peptides and small proteins, such as insulin, to pass through its network to release, but retain the bacteria particles, if there are some, within the polymer matrix. This feature may simplify sterilization process by steaming the final product in an organic vapor, such as an oxirane–CO_2 mixture, for which the costly aseptic facilities for the entire process may be avoided.

Purple clay is a ceramic forming material having been used to make teapot in China for centuries. Purple clay teapot is a type of popular handicrafts for its ability to hold teas (water impermeable) and breath (air permeable). We used purple

© 2015 WILEY-VCH Verlag GmbH & Co. KGaA, Weinheim

clay for its easiness in manual fabricating the molds. Even if the purple clay may not be the optimal material for making microneedle molds, the concept of using an air permeable but water impermeable mold to scale up the fabrication process is feasible and practical.

4. Conclusions

The PTM patch described herein overcomes two limitations associated with DMs and hydrogel-forming microneedles, respectively, deposition of needle tip materials in the skin and inability to load insulin safely in the matrix of the needle tips to achieve sufficient efficacy. The water swellable-but-insoluble nature of PTM ensures efficient *trans*-epidermal delivery of insulin and sufficient mechanical strength at hydrated state for complete withdraw without depositing excess materials. The antidissolution cross-linking of the microneedle matrix of PTM is achieved by microcrystalline domains as the cross-linking junctions via a mild freeze-thaw treatment, for which insulin may safely be loaded in the matrix of the microneedle tips to ensure sufficient hypoglycemic efficacy. The fabrication process involving an air-permeable but water-impermeable mold is scalable for cost-efficient production due to two features: 1) the freeze-thawed microneedle sheets are sufficiently strong to be detached and release the molds to the production cycle; and 2) sterilization may be achieved by steaming the final products in an organic vapor to avoid costly aseptic facilities for the entire process. These design features of PTM render it a practically feasible noninjection delivery system for insulin.

5. Experimental Section

Fabrication Process of Phase Transition Microneedle (PTM) Patches: Fabrication of phase transition microneedle patches started with preparation of a ceramic mold which is permeable to air but not water. A ceramic-forming material named purple clay was used to form the mold for its believed "breathability (permeable to air)." A purple clay dough was impressed by a male mold, dried in air, and calcinated at 1000 °C. To form the microneedle patch, an insulin-loaded aqueous solution containing PVA (as the main component) and polysaccharides was casted on the mold and socked into the microholes by applying vacuum on the back side of the mold. Then a preformed PVA hydrogel plate was placed on the top of the casted solution, followed by a freeze-thaw treatment to allow the PVA solution to form microcrystalline domains as the cross-linking junctions.[31] The well-gelled microneedle sheet was detached from the mold and dried in air under a mechanic guidance to avoid curling. Finally, the dried microneedle sheet was punched to patches of designed size. Insulin content in each PTM patch was determined by extracting all insulin of a patch using 200 mL phosphoric acid buffer (pH2) and measuring the solution using HPLC (Agilent, USA) equipped with a C-18 column.

Mechanic Strength of PTM Microneedles: To evaluate resistance to static force, microneedle patches made of the present composition as well as those made of hyaluronic acid (HA) and carboxymethylcellulose (CMC) were cut to the size of 5 mm × 6 mm (26 mm^2 in area and 30 needle tips) and placed on a stainless steel plate with the needle tips facedown. Weights of 100, 230, 330, and 460 g were placed on the top of each patch successively and gently. To assess resistance to dynamic impact, the microneedle patches being examined (same size as above) were placed on the stainless steel plate with the needle tips face-up. Weights of 10, 20, and 50 g were dropped on to the top of each patch from a height of 20 mm. The microneedle patches were examined using a magnifier after being pressed or hit by each of the weights for the failure of the needle tips. If failure of the needle tips was identified, the patches were cut to strip with a line of the microneedles and imaged for the side view of the needle tips under a microscope (Olympus CX41).

Microneedle Swelling and Live Skin Recovery: Swelling of the microneedles of the PTM patches by body fluid is examined on several human volunteers of mixed sexes under an approval of the internal institutional committee. To confirm whether the microneedles were swollen by the body fluid in the dermis layer or by sweat, two drug-free patches with and without microneedles were applied on the skin of each of the three volunteers. The two patches were from the same batch (the same microneedle sheet), one of which the needle tips were excised prior to application. The spot of the skin for receiving microneedle patches was clean with 75% alcohol, and the patches (113 mm^2 in area that holds ≈135 needle tips) were pressed by thumb (a force of 2.0–2.5 kg) and held on the skin spot by an adhesive backing membrane from 3M (9860, 3M, USA; also see Figure 2). The force used to impress the microneedles was measured using a weighting meter. A volunteer placed an arm on the meter and pressed a PTM patch on top of the arm and read the meter. The two patches were removed from the skin 3 h later and photographed immediately using a camera (Sp-565uz, Olympus, JP). For comparison, a microneedle patch not applied on skin was imaged as well. The skin spot received microneedle patch was imaged as a function of time after removal of the patch (Figure 2).

Pharmacokinetics: Three groups of normal pigs ($n = 6$) were given three different doses of the insulin-loaded PTM in the form of 1 (1.0 IU kg^{-1}), 2 (2.0 IU kg^{-1}), and 3 (3.0 IU kg^{-1}) patches, respectively. The patches were held on the skin of the ears of the pigs with an adhesive backing membrane (9860, 3M, USA) for 480 min. The hairs on the pig ears had been gently shaved using a shaver for human. For comparison, another group of normal pigs received subcutaneous injection by insulin pen (0.4 IU kg^{-1}). Blood samples were taken from the pigs at each programmed data point, −60, −40, −20, 0, 10, 20, 30, 45, 60, 90, 120, 180, 240, 300, 360, 420, and 480 min, after administration, assayed using the ELISA kit as above, and plotted against time after subtracting the baseline value. Based on the result for the normal pigs, two groups of diabetic pigs were administrated by subcutaneous injection (0.4IU kg^{-1}) and with two microneedle patches (2.0 IU kg^{-1}), respectively, for determination of relative bioavailability. Sampling and data analysis for the diabetic pigs were the same as for the normal pigs.

Efficacy of Insulin PTM in Pig Models: The efficacy study was carried out on diabetic pig models, while both normal and diabetic pigs were used for pharmacokinetic experiments. The diabetic pigs were prepared by removing 75% of the pancreas by an experienced surgical doctor. Prior to surgical operation, the pigs were anesthetized by intravenous injection of sodium pentobarbital (30 mg kg^{-1}) and fixed on operating tables. The pigs receiving surgical operation were carefully monitored for 2 weeks during which time the blood sugar was measured in 2 d intervals using blood sugar monitor (ACCU-CHEK, Roche, CH). Those animals with blood sugar stabilized above 17 mmol L^{-1} were selected for the pharmacokinetics and efficacy (PD/PK) study. For most of the pig models, the basal blood glucose level was around 19 mmol L^{-1} during the 2 weeks observation period. The efficacy of the insulin microneedle patch was examined by measuring the blood sugar changes before and after insulin administration in fasted and glucose-injected model pigs, as well as by measuring glycated hemoglobin level for the pigs treated continuously with the insulin dosage forms for 2 months. For blood sugar changes, the diabetic pigs, 11–12 kg in body weight, were divided into five groups to receive no insulin treatment, 0.4 IU kg^{-1} injection pen, and 1 (1.0 IU kg^{-1}), 2 (2.0 IU kg^{-1}), and 3 (IU kg^{-1}) microneedle patches, respectively. The microneedle patches were pressed and immobilized on the skin of ears of the pigs, where hairs were removed gently in advance using a shaver for human. For the fasted (12 h) pigs, blood sugar of all the pigs was determined at 0 and 2 h after insulin administration. For the feed pigs (injected with 0.6 g kg^{-1} glucose prior to giving insulin), blood sugar was determined at 0, 0.5, 1, 2, and 3 h since the insulin administration.

© 2015 WILEY-VCH Verlag GmbH & Co. KGaA, Weinheim

Measurement of Glycated Hemoglobin: For evaluating the efficacy of PTM patches in long-term blood sugar control, the diabetic pigs were continuously given injection pen (0.4 IU kg^{-1}) and microneedle patch (2.0 IU kg^{-1}), twice a day and 8 h in interval for 2 months. Glycated hemoglobin (HbA1c) was determined by centrifuging (1000 rpm for 10 min) and rinsing the blood samples collected from the 2 month treatment pigs, followed by hemolysis, acidizing, and hydrolysis. The content of HbA1c (mmol mol^{-1}) was calculated based on the absorbance at 450 nm recorded on an ELISA reader.

Insulin Stability and Bioactivity in Different Dosage Forms: To examine the resistance of the insulin patch to heat, an important criterion for biologic medicines in daily application, we baked the patches, together with the solution form of insulin (Humalog-100 IU mL^{-1}, Lilly, USA), at 60 °C for 72 h. Both of the injection pen and the microneedle patches were sealed in each tube and shacked in an oven (HZQ-F160, Hualong, CN) at 100 rpm. The improvement of insulin stability by the patch matrix was evaluated by the changes in insulin content and hypoglycemic activity. For the content and activity measurement, the solution dosage form was taken out after 0, 2, 4, 6, 8, 10, 12, 24, 48, and 72 h of baking, and diluted to ≈0.1 IU mL^{-1} with a phosphoric acid buffer of pH2. The microneedle patches were baked for 0, 24, 48, and 72 h, followed by insulin extraction using 200 mL phosphoric acid buffer (pH2) per patch. The insulin content of both injection pen and patch extracts was measured using HPLC (Agilent, USA) equipped with a C-18 column. The mobile phase consists 28 g L^{-1} Na_2SO_4 dissolved in a mixed solvent of water and acetonitrile (74:26) at pH 2.3, and running at a flow rate of 1mL min^{-1}. The column temperature was 40 °C and the detection wave length was 216 nm. The changes in hypoglycemic activity by baking was examined by injecting fresh insulin solution and of the insulin extracts from baked and unbaked microneedle patches to three groups of normal mice (20 g in body weight, 10 in each group) at the dose of 1.0 IU kg^{-1}. Blood sugar in the mice was measured before and 40 min after the insulin administration.

Animal Welfare and Experiment Ethical Issues: The pig experiments and the human skin recovery tests were carried out with the consent of the internal experiment ethic committee of the school.

Acknowledgements

T.J. invented the initial idea, designed the experiments with S.Y., carried out the hardness test, and finalized the manuscript. S.Y. carried out the experiments and drafted the manuscript. F.W. repeated and confirmed some key results. J.L. and G.F. designed and instructed the efficacy and PK experiments. W.Y. and H.Z. involved in discussion. This work was financially supported by the National Grand New Drug Program of China (No. 2009ZX09310-007), the National Nature Science Foundation of China (No. 81173001), and BioPharm Solutions, Inc.

Received: February 9, 2015
Published online: June 18, 2015

[1] S. Heller, P. Kozlovski, P. Kurtzhals, *Diabetes Res. Clin. Pr.* **2007**, *78*, 149.
[2] C. Damgé, P. Maincent, N. Ubrich, *J. Controlled Release* **2007**, *117*, 163.
[3] A. Barnett, *Int. J. Clin. Pract.* **2004**, *58*, 394.
[4] P. S. Odegard, K. L. Capoccia, *Ann. Pharmacother.* **2005**, *39*, 843.
[5] M. Morishita, T. Goto, N. A. Peppas, J. I. Joseph, M. C. Torjman, C. Munsick, K. Nakamura, T. Yamagata, K. Takayama, A. M. Lowman, *J. Controlled Release* **2004**, *97*, 115.
[6] D. L. Bremseth, F. Pass, *Diabetes Technol. Ther.* **2001**, *3*, 225.
[7] S. Andrews, J. W. Lee, S. O. Choi, M. R. Prausnitz, *Pharm. Res.* **2011**, *28*, 2110.
[8] S. Henry, D. V. McAllister, M. G. Allen, M. R. Prausnitz, *J. Pharm. Sci.* **1998**, *87*, 922.
[9] F. Wu, S. Yang, W. Yuan, T. Jin, *Curr. Pharm. Biotechnol.* **2012**, *13*, 1292.
[10] M. R. Prausnitz, *Adv. Drug Delivery Rev.* **2004**, *56*, 581.
[11] L. Lin, A. P. Pisano, *J. Microelectromech. Syst.* **1999**, *8*, 78.
[12] T. Omatsu, K. Chujo, K. Miyamoto, M. Okida, K. Nakamura, N. Aoki, R. Morita, *Opt. Express* **2010**, *18*, 17967.
[13] M. Cormier, B. Johnson, M. Ameri, K. Nyam, L. Libiran, D. D. Zhang, P. Daddona, *J. Controlled Release* **2004**, *97*, 503.
[14] S. P. Davis, W. Martanto, M. G. Allen, M. R. Prausnitz, *IEEE Trans. Biomed. Eng.* **2005**, *52*, 909.
[15] P. M. Wang, M. Cornwell, J. Hill, M. R. Prausnitz, *J. Invest. Dermatol.* **2006**, *126*, 1080.
[16] S. P. Sullivan, D. G. Koutsonanos, M. del Pilar Martin, J. W. Lee, V. Zarnitsyn, S. O. Choi, N. Murthy, R. W. Compans, I. Skountzou, M. R. Prausnitz, *Nat. Med.* **2010**, *16*, 915.
[17] J. W. Lee, J. H. Park, M. R. Prausnitz, *Biomaterials* **2008**, *29*, 2113.
[18] J. J. Norman, M. R. Brown, N. A. Raviele, M. R. Prausnitz, E. I. Felner, *Pediatr. Diabetes* **2013**, *14*, 459.
[19] P. C. Demuth, Y. Min, B. Huang, J. A. Kramer, A. D. Miller, D. H. Barouch, P. T. Hammond, D. J. Irvine, *Nat. Mater.* **2013**, *12*, 367.
[20] S. Liu, Y. S. Quan, F. Kamiyama, L. Fang, A. Yamamoto, *J. Shenyang Pharm. Univ.* **2010**, *27*, 6.
[21] S. Liu, M. N. Jin, Y. S. Quan, F. Kamiyama, H. Katsumi, T. Sakane, A. Yamamoto, *J. Controlled Release* **2012**, *161*, 933.
[22] R. F. Donnelly, T. R. R. Singh, M. J. Garland, K. Migalska, R. Majithiya, C. M. McCrudden, P. L. Kole, T. M. T. Mahmood, H. O. McCarthy, A. D. Woolfson, *Adv. Funct. Mater.* **2012**, *22*, 4879.
[23] A. D. Woolfson, D. J. Morrow, A. Morrissey, R. F. Donnelly, P. A. Mccarron, *WO2009040548*, **2009**.
[24] C. M. Hassan, N. A. Peppas, *Macromolecules* **2000**, *33*, 2472.
[25] U. Fumio, Y. Hiroshi, N. Kumiko, N. Sachihiko, S. Kenji, M. Yasunori, *Int. J. Pharm.* **1990**, *58*, 135.
[26] T. Jin, *WO2010040271*, **2009**.
[27] Y. Ito, T. Yamazaki, N. Sugioka, K. Takada, *J. Mater. Sci. Mater. Med.* **2010**, *21*, 835.
[28] N. A. Peppas, E. W. Merrill, *J. Appl. Polym. Sci.* **1977**, *21*, 1763.
[29] M. I. Baker, S. P. Walsh, Z. Schwartz, B. D. Boyan, *J. Biomed. Mater. Res. B: Appl. Biomater.* **2012**, *100*, 1451.
[30] Y. Sakurada, A. Sueoka, M. Kawahashi, *Polym. J.* **1987**, *19*, 501.
[31] S. Yang, Y. Feng, L. Zhang, N. Chen, W. Yuan, T. Jin, *Int. J. Nanomedicine* **2012**, *7*, 1415.

© 2015 WILEY-VCH Verlag GmbH & Co. KGaA, Weinheim